Title
Imaging shear wave propagation for elastic measurement using OCT Doppler variance method

ISBN
9781628419313

Authors
Zhu, Jiang
Miao, Yusi
Qu, Yueqiao
et al.

Publication Date
2016-03-08

DOI
10.1117/12.2214266

Imaging shear wave propagation for elastic measurement using OCT Doppler variance method

Jiang Zhu[*,a],Yusi Miao[*,a,b], Yueqiao Qu[a,b] , Teng Ma[c] , Rui Li[a] , Yongzhao Du[a], Shenghai Huang[a], K. Kirk Shung[c], Qifa Zhou[c], and Zhongping Chen[a,b,+]

[a] Beckman Laser Institute, University of California, Irvine, Irvine, California 92612; [b] Department of Biomedical Engineering, University of California, Irvine, Irvine, California 92697; [c] Department of Biomedical Engineering, University of Southern California, Los Angeles, California 90089

ABSTRACT

In this study, we have developed an acoustic radiation force orthogonal excitation optical coherence elastography (ARFOE-OCE) method for the visualization of the shear wave and the calculation of the shear modulus based on the OCT Doppler variance method. The vibration perpendicular to the OCT detection direction is induced by the remote acoustic radiation force (ARF) and the shear wave propagating along the OCT beam is visualized by the OCT M-scan. The homogeneous agar phantom and two-layer agar phantom are measured using the ARFOE-OCE system. The results show that the ARFOE-OCE system has the ability to measure the shear modulus beyond the OCT imaging depth. The OCT Doppler variance method, instead of the OCT Doppler phase method, is used for vibration detection without the need of high phase stability and phase wrapping correction. An M-scan instead of the B-scan for the visualization of the shear wave also simplifies the data processing.

Keywords: Optical coherence tomography, OCT Doppler variance, Optical coherence elastography, Acoustic radiation force, Shear wave.

[*]First two authors contributed equally to this work
[+]Corresponding author: z2chen@uci.edu

1. INTRODUCTION

Elastography is an imaging modality for the measurement of elastic properties. Clinically, the elastic properties of soft tissues are associated with the status of diseases. Elastography based on nuclear magnetic resonance imaging, ultrasonography and optical coherence tomography has been developed. Compared with magnetic resonance elastography[1] and ultrasound elastography,[2,3] optical coherence elastography (OCE) has a much higher spatial resolution.[4] Because mechanical properties of living tissues are critical indicators of tissue pathological conditions, OCE offers great potentials for diagnosis of cardiovascular and ocular diseases.

OCE utilizes the OCT unit for detection of elastic vibration. However, different excitation techniques have been employed to generate an elastic wave in tissues, such as the non-contact focused air-puff device,[5,6] ultrasonic transducer,[7-9] and a piezoelectric actuator.[10-12] In order to detect elastic properties of an internal tissue, the acoustic radiation force (ARF) has a greater advantage since it focuses on the deeper tissue and remotely induces the vibration.

In a previous ARF-OCE system, the acoustic force was parallel to the OCT detection direction. The vibration parallel to the OCT beam was detected by a Doppler phase method and the shear wave propagation perpendicular to the OCT beam was visualized by a B-scan.[13,14] The alignment of the ultrasound focus and OCT focus was difficult if the ultrasound transducer and OCT lens were located on the same side of the sample. The Doppler phase detection required high stability and may have been distorted by phase wrapping. Moreover, this method could only detect the elastic properties in the shallow part of the sample due to the limits of the OCT imaging depth.

To overcome these limitations, we developed the ARFOE-OCE method, where the acoustic force is orthogonal to the OCT detection direction, the vibration perpendicular to the OCT beam is detected by a Doppler variance method instead of a Doppler phase method, and a shear wave is visualized by a simple M-scan during propagating from the ARF focus to the sample surface. The ARFOE-OCE system can stably measure the shear wave velocity with a simpler procedure without the need of high OCT phase stability; it measures the shear wave velocity at different depths within a location by using an

Optical Coherence Tomography and Coherence Domain Optical Methods in Biomedicine XX, edited by Joseph A. Izatt, James G. Fujimoto, Valery V. Tuchin, Proc. of SPIE Vol. 9697, 96971P · © 2016 SPIE · CCC code: 1605-7422/16/$18 · doi: 10.1117/12.2214266

M-scan. Moreover, by changing the ARF focus to a deeper axial position and measuring the time delay of the transverse vibration due to wave propagation, we can quantitatively estimate the shear modulus at a position beyond the OCT imaging depth. Therefore, the detection depth for the elastic modulus of the ARFOE-OCE system is much deeper than previous OCE methods.

2. METHODOLOGY

2.1 ARFOE-OCE System

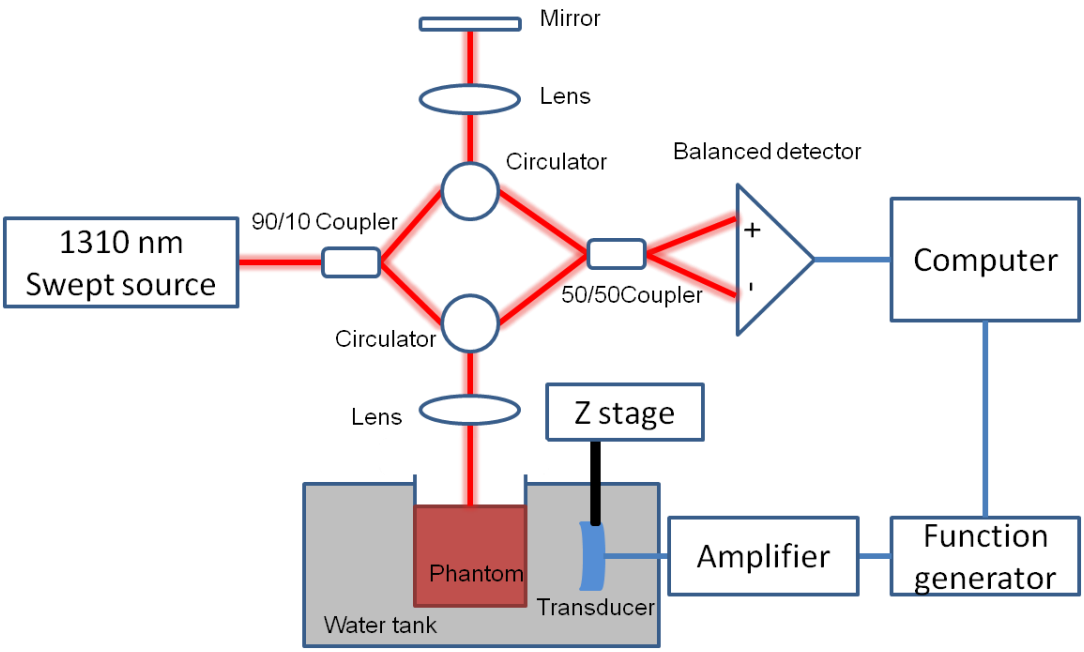

Figure 1. Schematic of the ARFOE-OCE system including an OCT imaging unit and an ultrasound excitation unit. The acoustic radiation direction is perpendicular to the optical detection direction.

A schematic of the ARFOE-OCE system is shown in Figure 1. The ARFOE-OCE system contains an OCT imaging unit and an ultrasound excitation unit. For ARF generation, an ultrasonic transducer is driven by the amplified sine wave with the frequency of 4.5 MHz. The swept source OCT system with a central wavelength of 1310 nm and an A-line speed of 50 kHz is used for the OCT imaging. Ninety percent of the light form laser goes to the sample arm and the other ten percent goes to the reference arm. In the sample arm, after the light passes through a galvo scanning mirror, low-coherent light is focused on the phantom through a scan lens. A dual-balanced detection scheme is adopted to obtain the signal. The tissue-equivalent phantom is placed in a container with a thin-film window for the ultrasound pass. The thin-film container and ultrasound transducer are immersed in water. For detection of the shear wave, the OCT M-scan, including 2000 A-lines at a rate of 50 kHz, takes a total 40.0 ms during which the ultrasound transducer generates two bursts of 1.0 ms for ARF excitation at the 1st A-line and at the 1001 A-line, respectively, as two repeats of the measurement. The acoustic radiation direction is perpendicular to the OCT detection direction.[15]

2.2 Doppler Variance Method

Doppler variance methods can be employed to extract the vibration information in transverse direction from OCT data.[16-19] Both intensity-based Doppler variance (IBDV) and phase-resolved Doppler variance methods can be used to measure the transverse vibration. Here, the IBDV method is used to explain the measurement principle, since both IBDV and phase-resolved Doppler variance methods provide similar results.

In the IBDV method, the vibration intensity is directly related to the intensity-based variance σ^2, which is calculated by the following equation:

$$\sigma_{j,i}^2 = 1 - \frac{2 \cdot |F_{j,i}| \cdot |F_{j+1,i}|}{F_{j,i} \cdot F^*_{j,i} + F_{j+1,i} \cdot F^*_{j+1,i}} \quad (1)$$

where $\sigma_{j,i}^2$ is the variance at j_{th} A line and i_{th} depth, and $F_{j,i}$ is the complex signal at j_{th} A-line and i_{th} depth. Unlike the Doppler phase method, the phase term is removed from the variance method so it can eliminate the distortion due to phase fluctuation. Furthermore, no phase wrapping correction is required for the variance method, and thus, the data processing is simplified.

2.3 Stiffness Estimation

After the visualization of the shear wave propagation, the shear modulus μ can be calculated from the shear wave velocity V with the following equation:

$$\mu_{x,z} = \rho \cdot V_{x,z}^2 \quad (2)$$

where $\mu_{x,z}$ is the shear modulus and $V_{x,z}^2$ is the propagation velocity of the shear wave at the lateral location x and the depth z. ρ is the density of the tissue-equivalent phantom.

Since the soft tissue is nearly incompressive, Poisson's ratio can be considered as 0.5. Therefore, the relationship between the shear modulus and Young's modulus is provided by the following equation:

$$E_{x,z} = 3 \cdot \mu_{x,z} . \quad (3)$$

3. RESULTS AND DISCUSSION

Using the ARFOE-OCE system, we first measured the shear wave velocity in a homogeneous 0.6% agar phantom. In order to measure the shear modulus beyond the OCT imaging depth, which could not be achieved by previous methods, we moved the transducer downward with a known step ΔD by a mechanical Z stage and then measured the time delay (T2-T1) for the wave arriving at the same observation point in the OCT imaging area. The schematic of the measurement method is shown in Fig. 2. After the ARF excitation of 1.0 ms, the induced vibration propagated from the ARF focus to the surface of the phantom in the Doppler variance image. The average shear wave velocity V between the two ARF positions, which are beyond the OCT imaging depth, can be determined by the following equation:

$$V = (\Delta D)/(T1 - T2) \quad (4)$$

where *T1* and *T2* are the propagation time of elastic wave to the OCT observation point from the upper ARF focus position and lower ARF focus position, respectively. ΔD is the distance between the upper ARF focus and lower ARF focus.

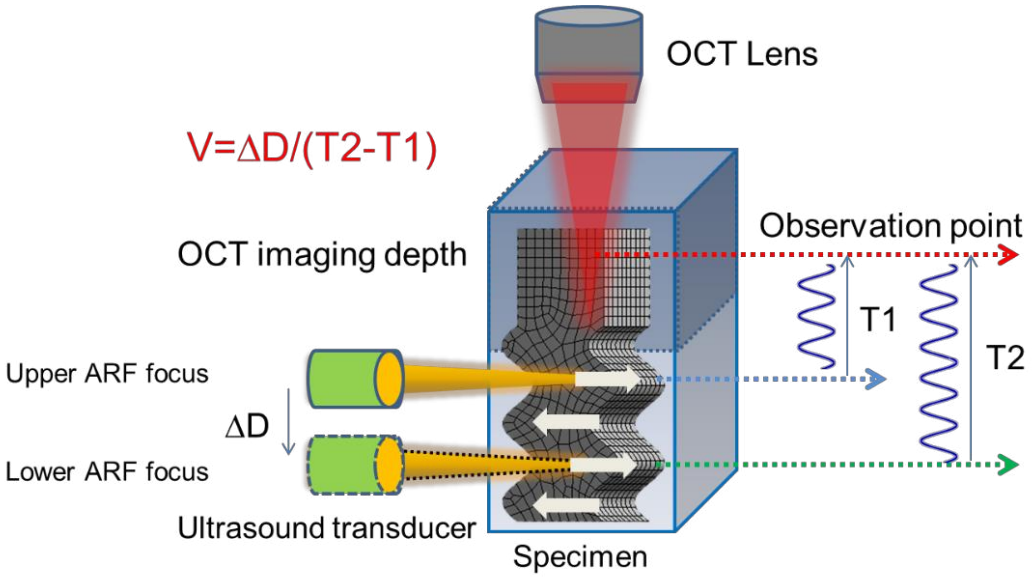

Figure 2. Shear wave measurement for a deeper phantom.

In Figure 3, the time delay for the wave arriving at the surface can be detected when the ARF focus is moved downward. Right shifts of the vibrations can be observed when the transducer is moved downward because the vibrations will be delayed when the shear wave travels a longer distance. The velocity of shear wave propagating from a lower ARF focus position to an upper ARF focus position is equal to 1.1 m/s for 0.6% agar phantom. The corresponding shear modulus calculated is 1.2 kPa. The detection depth depends on the shear wave attenuation and the OCT system sensitivity. By moving the ARF positions and detecting the time delay, the OCE measurement depth extends beyond the OCT imaging depth.

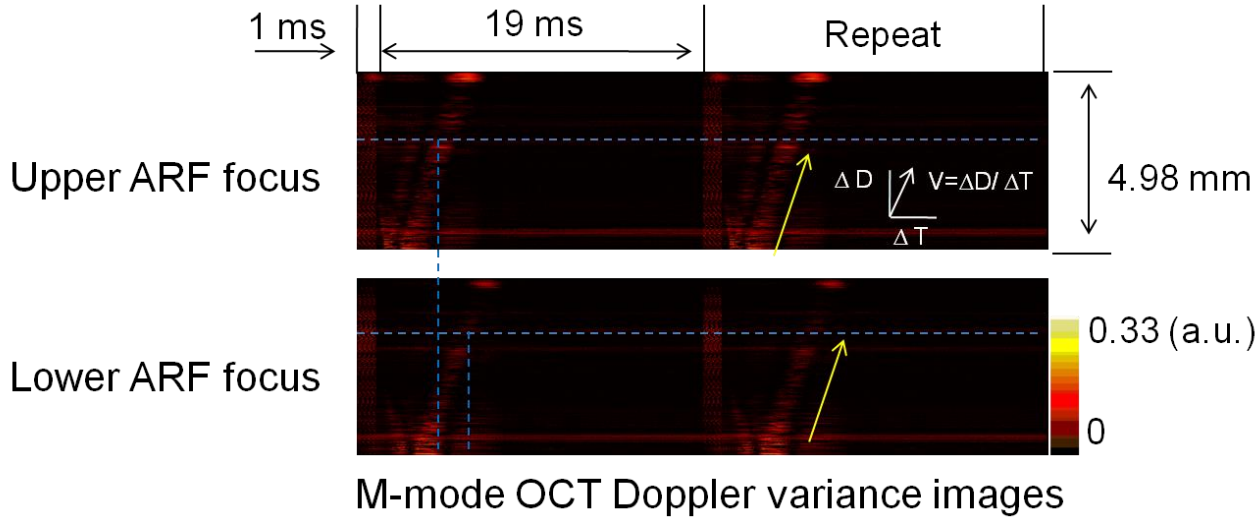

Figure 3. M-mode OCT Doppler variance images for shear wave measurement with different ARF focus excitation. (a) Shear wave propagation from upper ARF focus and (b) lower ARF focus.

Next, we measured the shear wave velocity in a two-layer agar phantom. Figure 4 shows the shear wave propagation in a two-layer phantom where the top layer contains 0.6% agar and the bottom layer contains 0.8% agar. Figure 4 shows the Doppler variance image and OCT image in M-mode. No obvious interface can be observed in the OCT image; however, an immediate change of shear wave velocity can be measured between the two layers from the Doppler variance image. The calculated shear velocity is 1.2 m/s for the top layer and 2.6 m/s for the bottom layer.

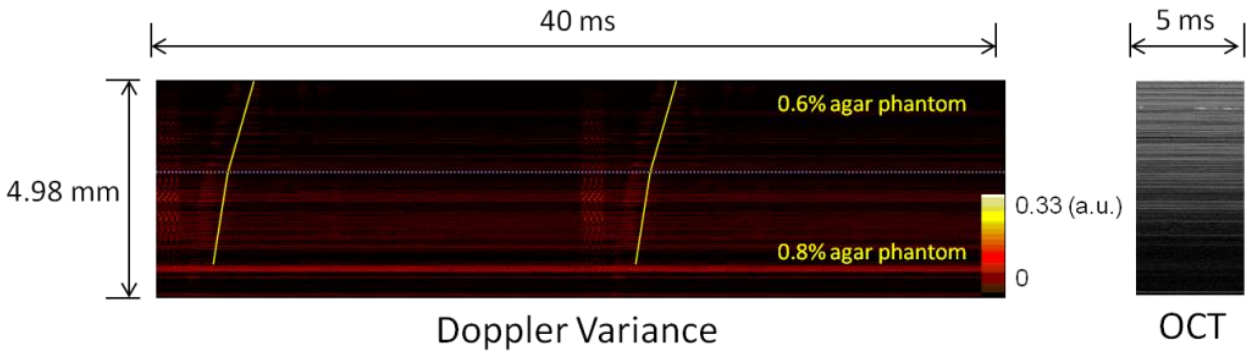

Figure 4. Visualization of the shear wave using an M-scan in a two-layer phantom.

4. CONCLUSION

In this study, we developed an ARFOE-OCE method for the measurement of shear wave velocity. This system can measure the shear modulus beyond the OCT imaging depth. A Doppler variance method used for the detection of sample vibration in this system doesn't require high OCT phase stability. Using an M-scan instead of a B-scan for visualization of the shear wave also simplifies the data processing. Using this system, we directly measured the propagation velocity of the shear wave at different depths of one location with an M-scan. By moving the ARF focus to a deeper position and measuring the time delay of detected transverse vibration, we can calculate the shear modulus beyond the OCT imaging depth.

ACKNOWLEDGMENTS

This work was supported by the National Institutes of Health under grants R01HL-127271, R01HL-125084, R01HL-105215, R01EY-021529, P41-EB002182, P41-EB015890. Dr. Zhongping Chen has a financial interest in OCT Medical Inc, which, however, did not support this work.

REFERENCES

[1] Muthupillai, R., Lomas, D., Rossman, P., Greenleaf, J., Manduca, A., Ehman, R., "Magnetic resonance elastography by direct visualization of propagating acoustic strain waves," Science 269(5232), 1854–1857 (1995).
[2] Nightingale, K., Mcaleavey, S., Trahey, G., "Shear-wave generation using acoustic radiation force: in vivo and ex vivo results," Ultrasound in Medicine & Biology 29(12), 1715–1723 (2003)
[3] Ma, T., Qian, X., Chiu, C. T., Yu, M., Jung, H., Tung, Y.-S., Shung, K. K., and Zhou, Q., "High-resolution harmonic motion imaging (HR-HMI) for tissue biomechanical property characterization," Quant. Imaging Med. Surg. 5(1), 108–117 (2015).
[4] Schmitt, J., "OCT elastography: imaging microscopic deformation and strain of tissue," Opt. Express 3(6), 199 (1998).
[5] Wang, S., Larin, K. V., "Shear wave imaging optical coherence tomography (SWI-OCT) for ocular tissue biomechanics," Opt. Lett. 39(1), 41 (2013).
[6] Wang, S., Lopez, A. L., Morikawa, Y., Tao, G., Li, J., Larina, I. V., Martin, J. F., Larin, K. V., "Noncontact quantitative biomechanical characterization of cardiac muscle using shear wave imaging optical coherence tomography," Biomed. Opt. Express 5(7), 1980 (2014).
[7] Nguyen, T.-M., Song, S., Arnal, B., Huang, Z., O'Donnell, M., Wang, R. K., "Visualizing ultrasonically induced shear wave propagation using phase-sensitive optical coherence tomography for dynamic elastography," Opt. Lett. 39(4), 838 (2014).
[8] Qi, W., Li, R., Ma, T., Shung, K. K., Zhou, Q., Chen, Z., "Confocal acoustic radiation force optical coherence elastography using a ring ultrasonic transducer," Appl. Phys. Lett. 104(12), 123702 (2014).
[9] Wu, C., Han, Z., Wang, S., Li, J., Singh, M., Liu, C.-H., Aglyamov, S., Emelianov, S., Manns, F., et al., "Assessing age-related changes in the biomechanical properties of rabbit lens using a coaligned ultrasound and optical coherence elastography system," Investigative Ophthalmology & Visual Science 56(2), 1292–1300 (2015).
[10] Liang, X., Oldenburg, A. L., Crecea, V., Chaney, E. J., Boppart, S. A., "Optical micro-scale mapping of dynamic biomechanical tissue properties," Opt. Express 16(15), 11052 (2008).

[11] Kennedy, B. F., Liang, X., Adie, S. G., Gerstmann, D. K., Quirk, B. C., Boppart, S. A., Sampson, D. D., "In vivo three-dimensional optical coherence elastography," Opt. Express 19(7), 6623 (2011).
[12] Song, S., Huang, Z., Nguyen, T.-M., Wong, E. Y., Arnal, B., O'Donnell, M., Wang, R. K., "Shear modulus imaging by direct visualization of propagating shear waves with phase-sensitive optical coherence tomography," J. Biomed. Opt 18(12), 121509 (2013).
[13] Nguyen, T.-M., Arnal, B., Song, S., Huang, Z., Wang, R. K., O'Donnell, M., "Shear wave elastography using amplitude-modulated acoustic radiation force and phase-sensitive optical coherence tomography," J. Biomed. Opt 20(1), 016001 (2015).
[14] Nguyen, T.-M., Song, S., Arnal, B., Huang, Z., O'Donnell, M., Wang, R. K., "Visualizing ultrasonically induced shear wave propagation using phase-sensitive optical coherence tomography for dynamic elastography," Opt. Lett. 39(4), 838 (2014).
[15] Zhu, J., Qu, Y., Ma, T., Li, R., Du, Y., Huang, S., Shung, K. K., Zhou, Q., Chen, Z., "Imaging and characterizing shear wave and shear modulus under orthogonal acoustic radiation force excitation using OCT Doppler variance method," Opt. Lett. 40(9), 2099 (2015).
[16] Liu, G., Lin, A. J., Tromberg, B. J., Chen, Z., "A comparison of Doppler optical coherence tomography methods," Biomed. Opt. Express 3(10), 2669 (2012).
[17] Liu, G., Chou, L., Jia, W., Qi, W., Choi, B., Chen, Z., "Intensity-based modified Doppler variance algorithm: application to phase instable and phase stable optical coherence tomography systems," Opt. Express 19(12), 11429 (2011).
[18] Zhao, Y., Chen, Z., Saxer, C., Shen, Q., Xiang, S., Boer, J. F. D., Nelson, J. S., "Doppler standard deviation imaging for clinical monitoring of in vivo human skin blood flow," Opt. Lett. 25(18), 1358 (2000).
[19] Huang, S., Piao, Z., Zhu, J., Lu, F., Chen, Z., "In vivo microvascular network imaging of the human retina combined with an automatic three-dimensional segmentation method," J. Biomed. Opt 20(7), 076003 (2015).